The Folding of Triangulated Cylinders, Part I: Geometric Considerations

S. D. Guest

S. Pellegrino

Department of Engineering,
University of Cambridge,
Trumpington Street,
Cambridge, CB2 1PZ, U.K.

This study was inspired by a model of a triangulated cylindrical shell made by C. R. Calladine during an investigation of the mechanics of biological structures. The model consisted of identical triangular panels on a helical strip and had a small-displacement internal inextensional mechanism. It is shown that many triangulated cylinders broadly similar to Calladine's model can be folded down to a compact stack of plates: only small strains, whose magnitude can be made arbitrarily small by the choice of suitable design parameters, are imposed during folding. A general geometric formulation of the problem is presented and then, assuming that the folding process is uniform, the folding properties of any triangulated cylinder of this generic type are discussed.

1 Introduction and Some Simple Examples

The work described in this paper is part of a series of related projects in the area of deployable structures whose general aim is the development of simple and effective concepts. An overview of recent work in this field has been compiled by Kwan (1991); other concepts which have emerged from recent work at Cambridge can be seen in Kwan, You, and Pellegrino (1993) and Guest and Pellegrino (1992).

The present study was inspired by a cardboard model of a triangulated cylindrical shell made by C. R. Calladine during an investigation of the mechanics of biological structures. This model consisted of identical triangular panels on a helical strip and had a small-displacement internal inextensional mechanism. We decided to explore the possibility of transforming its small-displacement mechanism into a large-displacement motion by which a triangulated cylindrical shell could be folded down to a compact stack of plates. Quite quickly we found many arrangements that would allow this: only small strains, whose magnitude can be made as small as required by choosing suitable design parameters, are imposed during folding. Recently we have found a more general way of approaching the problem, which considers all possible triangulated cylinders of the same generic type.

In this paper, after describing the general configuration of a triangulated cylinder based on one or more helical strips, we identify those particular configurations which are suitable for folding. Our estimates of strain levels in the plates will be based on the simplifying assumptions that the folding process is uniform and that only one side of each triangle can change its length. Based on the insight gained from this approach, in a separate paper (Guest and Pellegrino, 1994) we have removed these assumptions and simulated the folding process of some particular cylinders. Before considering the fully general case in the next sections, we introduce the problem by discussing briefly some specific examples.

Figure 1 shows photographs of the folding of a particular triangulated cylinder when a flat plate on the top is gradually pushed down. In Fig. 1(*a*) the model is nearly fully extended; only a few triangular plates have been packaged. Then, as a small axial force is applied to the top plate, more and more triangles become part of the prismatic stack at the top of the cylinder and, in Fig. 1(*c*), only a few triangles are still extended. The packaged configuration of this particular cylinder is a heptagonal prism. All cylinders made from isosceles triangles, like this one, fold down to prisms. They are a special case for which the general parameter n—defined in Section 2—becomes equal to one plus the number of sides in the packaged configuration. Hence, the triangulated cylinder of Fig. 1 has $n = 8$.

In this paper it is assumed that the plates have negligible thicknesses.

Figure 2 shows line drawings of triangulated cylinders with $n = 6$, 7, and 8. As for all cylinders considered in this paper, they are *strain-free both in their fully extended and fully folded configurations*. In each cylinder all triangles are identical, and their sides are denoted by a, b, and c. These particular cylinders are made from isosceles triangles and hence their geometry is quite easy to analyze. For example, for $n = 7$ all corners of the triangles in the packaged configuration coincide with the corners of a hexagon, as shown in Fig. 2(*b.ii*). Thus, the lengths of sides a and b, $l_a = l_b$, are related to the length of side c, l_c, by the relationship

Contributed by the Applied Mechanics Division of THE AMERICAN SOCIETY OF MECHANICAL ENGINEERS for publication in the ASME JOURNAL OF APPLIED MECHANICS.

Discussion on this paper should be addressed to the Technical Editor, Professor Lewis T. Wheeler, Department of Mechanical Engineering, University of Houston, Houston, TX 77204-4792, and will be accepted until four months after final publication of the paper itself in the ASME JOURNAL OF APPLIED MECHANICS.

Manuscript received by the ASME Applied Mechanics Division, Aug. 13, 1992; final revision, Apr. 27, 1993. Associate Technical Editor: F. Y. M. Wan.

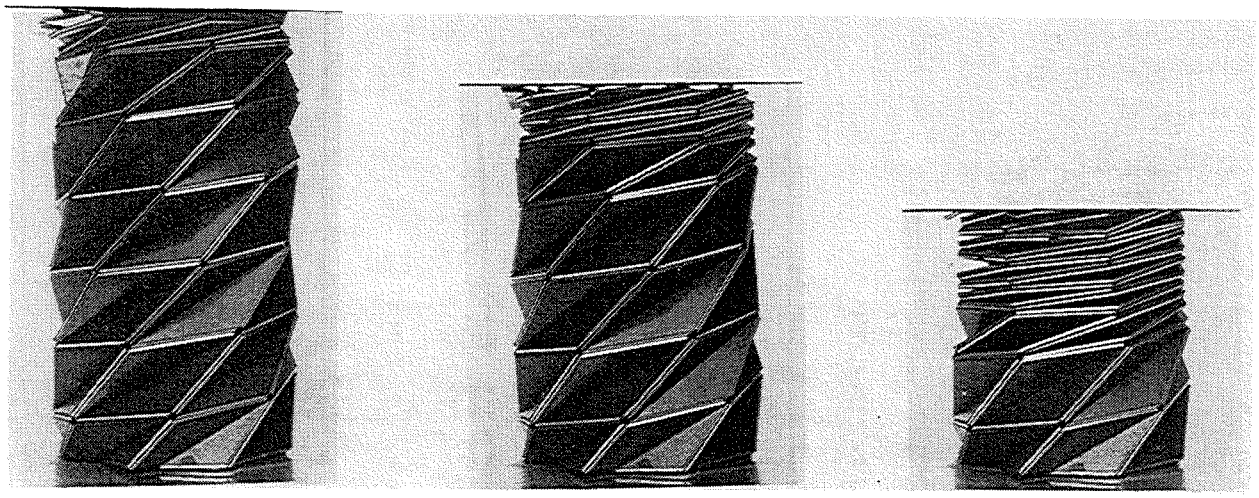

Fig. 1(*a*) Fig. 1(*b*) Fig. 1(*c*)

Fig. 1 Folding sequence of triangulated cylinders with $m=1$, $n=8$, $l_b/l_a=1$, $l_c/l_a=1.802$. The model shown has Al-alloy plates and flexible plastic hinges; its fully extended height is approximately 250 mm.

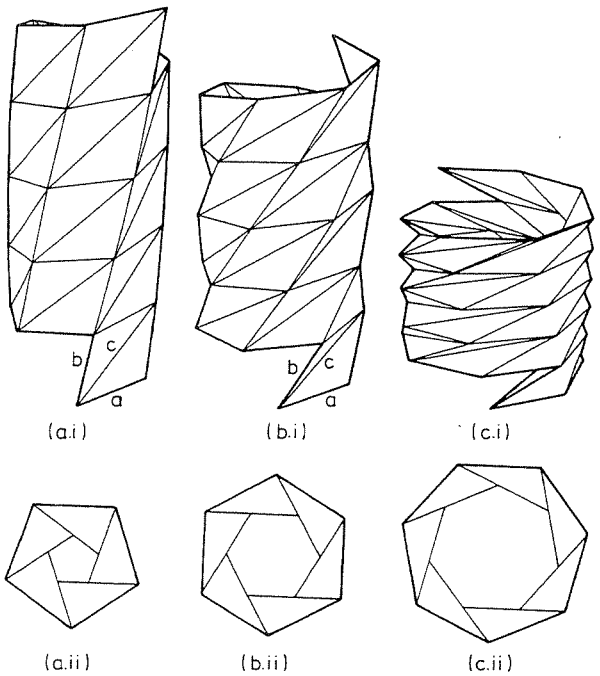

Fig. 2 Triangulated cylinders with $m=1$ and (*a*) $n=6$, (*b*) $n=7$, and (*c*) $n=8$. (*i*) Fully extended, side view. (*ii*) Fully folded, plan view. All cylinders have $l_b/l_a=1$.

$$l_c=2\sin\left(\frac{\pi}{2}-\frac{\pi}{n-1}\right)l_a=2\sin\left(\frac{\pi}{3}\right)l_a=\sqrt{3}\,l_a. \qquad (1)$$

To make a simple model of this cylinder, one draws on a sheet of thin card three sets of straight, parallel lines: the a and b lines are equi-distant and at an angle of $\pi/3$; the c lines go through the points of intersection of a and b lines. Then the sheet is folded along these lines: upwards along a and b lines, downwards along c lines. Finally, two opposite edges of the sheet are glued together to form the cylinder shown in Fig. 2(*b.i*). We have made card model cylinders of this sort for $n=7$, as described above, and also for $n=6$ and $n=8$. The axial force required to fold these models is quite small and the strains are sufficiently small that the models can survive substantially undamaged a small number of folding/unfolding cycles. However, it quickly becomes clear that the strains imposed by folding become lower as the value of n is increased. This observation has been confirmed by detailed computations (see Guest and Pellegrino, 1994) but now, having used these specific examples purely for illustration, we are ready to begin a proper investigation of the geometric design of triangulated cylinders, with the aim of identifying their folding properties.

The layout of the paper is as follows. Section 2 introduces the generic configuration in terms of three sets of helices lying on a cylindrical surface. These helices define the corners of the triangles forming the faceted cylinder. General expressions for the side lengths of the triangles are derived in terms of the helix parameters. With these tools, Section 3 examines the folding properties of a range of cylinders. Section 4 concludes the paper by discussing ways in which the results of Section 3 could be used to advantage in the design of foldable cylinders with different mechanical properties.

2 Geometry of Triangulated Cylinders

A general description of triangulated cylinders made from identical triangular plates arranged on helical strips, like those of Figs. 1 and 2, can be based on the observation that the nodes of the triangulated cylinders lie on the intersection of three sets of helices, as shown in Fig. 3. The helices are described by the sides of the triangles which are closest to them, i.e., they are called the a, b, and c helices.

All helices in one set are identical, apart from a rotation about the axis of the helix. A full set can be defined as a single helix with multiple starts. Each set of helices can be described by the following three parameters (Coxeter, 1980):

(*i*) the number of helices in the set, i.e., the number of starts of the helix (for example, in Fig. 3 the a helix has one start, the b helix seven starts, and the c helix eight starts);
(*ii*) the radius, which has the same value for all helices of Fig. 3 since they all lie on the same circular cylindrical surface;
(*iii*) the angle that the helix makes with a plane perpendicular to the axis of the helix. This angle can be greater than $\pi/2$, for a left-handed helix.

The positions of the nodes, and hence the configuration of a triangulated cylinder, are fully defined by any two of the three helices described above, as the third has to pass through the intersections of the other two. We shall use the a and b helices to describe a triangulated cylinder, therefore it is necessary to give the parameters defining these helices. They are

r = the radius;
α, β = the angles that the a and b helices, respectively, make with a plane perpendicular to their axis;

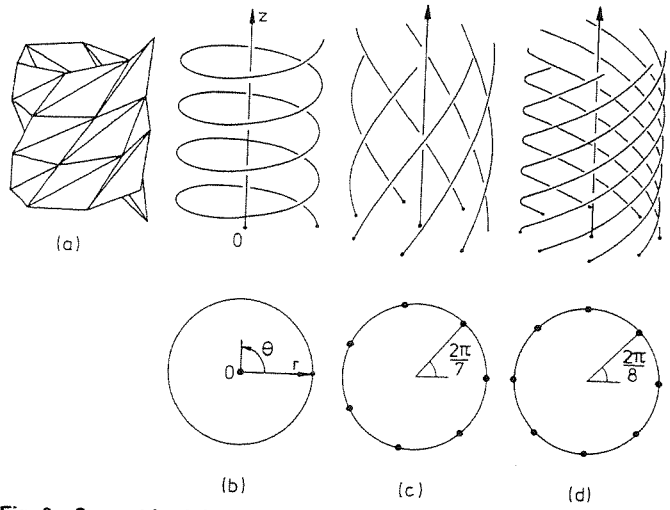

Fig. 3 Geometric definition of nodes of triangulated cylinder (*a*) in terms of three sets of helices, side, and plan views; (*b*) single-start *a*-helix, $m=1$; (*c*) seven-start *b*-helix, $n=7$; (*d*) eight-start *c*-helix, $m+n=8$. The first start of all helices is at (r, 0, 0).

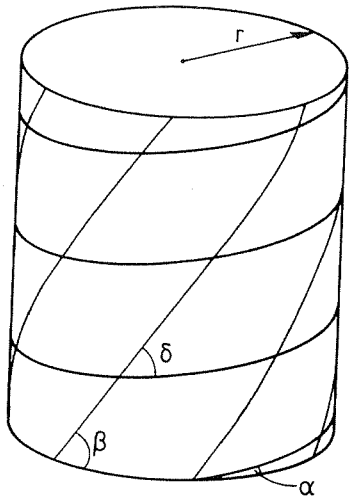

Fig. 4 Coordinate cylinder and parameters defining *a* and *b* helices

m, n = the number of starts of the a and b helices, respectively.

The parameters r, α, β are shown in Fig. 4. The a helix has the equation

$$z = r\theta \tan\alpha. \tag{2}$$

Similarly, the first start of the b helix is defined by

$$z = r\theta \tan\beta \tag{3}$$

and the second start by

$$z = r\left(\theta - \frac{2\pi}{n}\right)\tan\beta, \tag{4}$$

which gives $z=0$ when $\theta = 2\pi/n$. Note that in Eqs. (2)-(4) $0<\theta<+\infty$: a complete turn of a helix corresponds, obviously, to an increase in the value of θ by 2π.

We define a nodal numbering system where nodes are numbered along the a helices: node (i, j) is the jth node on the ith start of the a helix.

The next task is obtaining the coordinates of enough neighbors of node (1, 1) to be able to calculate the three side lengths of the triangles. The cylindrical coordinate system to be used, O, r, θ, z, is defined in Fig. 3(b): node (i, j) has coordinates $(r, \theta_{i,j}, z_{i,j})$. We define $\theta_{i,j}$ such that $0 \le \theta_{i,j} < 2\pi$ and hence

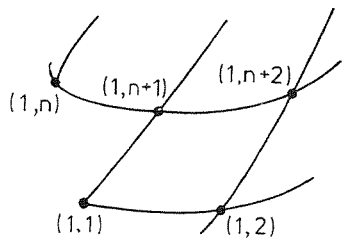

Fig. 5(*a*)

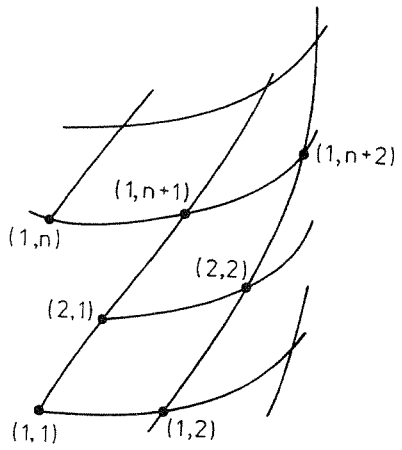

Fig. 5(*b*)

Fig. 5 Neighbors of mode (1,1) for a triangulated cylinder with (*a*) $m=1$ and (*b*) $m=2$. The *c* helices are not shown.

suitable multiples of 2π will be added to it when it is substituted into Eqs. (2)-(4). Node (1, 1) has coordinates (r, 0, 0).

For simplicity, the case $m=1$ will be considered first. Figure 5(a) shows that the θ-coordinates needed are those of nodes (1, 2), (1, $n+1$), and (1, $n+2$).

At node (1, 2) the a helix and the second start of the b helix intersect and so, from Eqs. (2) and (4),

$$r\theta_{1,2}\tan\alpha = r\left(\theta_{1,2} - \frac{2\pi}{n}\right)\tan\beta$$

which gives

$$\theta_{1,2} = \frac{2\pi}{n(1-k)} \tag{5}$$

where

$$k = \frac{\tan\alpha}{\tan\beta}. \tag{6}$$

At node (1, $n+1$) the second turn of the a helix and the first start of the b helix intersect and so, from Eqs. (2), (3)

$$r(\theta_{1,n+1} + 2\pi)\tan\alpha = r\theta_{1,n+1}\tan\beta$$

giving

$$\theta_{1,n+1} = \frac{2k\pi}{1-k}. \tag{7}$$

From Fig. 5(a), $\theta_{1,n+2} = \theta_{1,2} + \theta_{1,n+1}$ and therefore

$$\theta_{1,n+2} = \frac{2(1+kn)\pi}{n(1-k)}. \tag{8}$$

For cases where $m>1$ the nodes connected to node (1, 1) are those shown in Fig. 5(b). The expression for $\theta_{1,2}$ remains that of Eq. (5). The expression for $\theta_{1,n+1}$ does not change either, but it is now $\theta_{2,1}$ which is required, and so from Fig. 5(b)

$$\theta_{2,1} = \frac{\theta_{1,n+1}}{m} = \frac{2k\pi}{m(1-k)}. \tag{9}$$

Also

$$\theta_{2,2}=\theta_{1,2}+\theta_{2,1}=\frac{2(m+nk)\pi}{mn(1-k)}. \tag{10}$$

All relevant θ-coordinates are now defined. The next, final step is to calculate the side lengths l_a, l_b, and l_c in terms of the parameters defining the helices. In general, the distance l between node (1,1) and a node with coordinates (r, θ, z) is

$$l=\sqrt{\left(2r\sin\frac{\theta}{2}\right)^2+z^2}$$

For node (1,2), $l=l_a$, $\theta=\theta_{1,2}$, and—from Eq. (2)—$z=r\theta_{1,2}\tan\alpha$, hence

$$l_a=\sqrt{\left(2r\sin\frac{\pi}{n(1-k)}\right)^2+\left(\frac{2\pi r}{n(1-k)}\tan\alpha\right)^2}. \tag{11}$$

Similarly, for node $(1,n+1)$ if $m=1$, or node (2,1) if $m>1$, $l=l_b$ and $\theta=\theta_{1,n+1}$, or $l=l_b$ and $\theta=\theta_{2,1}$, respectively. The z-coordinate is

$$z=\frac{n}{m}z_{1,2}=\frac{n}{m}r\theta_{1,2}\tan\alpha$$

hence

$$l_b=\sqrt{\left(2r\sin\frac{k\pi}{m(1-k)}\right)^2+\left(\frac{2\pi r}{m(1-k)}\tan\alpha\right)^2}. \tag{12}$$

Similarly, for node $(1,n+2)$ if $m=1$, or node (2,2) if $m>1$, $l=l_c$ and $\theta=\theta_{1,n+2}$, or $l=l_c$ and $\theta=\theta_{2,2}$, respectively, and

$$z=\left(1+\frac{n}{m}\right)z_{1,2}=\frac{m+n}{m}r\theta_{1,2}\tan\alpha$$

hence

$$l_c=\sqrt{\left(2r\sin\frac{(m+nk)\pi}{mn(1-k)}\right)^2+\left(\frac{2(m+n)\pi r}{mn(1-k)}\tan\alpha\right)^2}. \tag{13}$$

Given the parameters which define the helices of a triangulated cylinder, it is possible to work out the side lengths of the triangular panels from Eqs. (11)-(13). Equally, it is possible to work backwards and, given a set of side lengths l_a, l_b, and l_c, and the topological parameters m, n, to work out the parameters of a corresponding set of helices.

There is one final condition, the inner edges of the triangles cannot cross the z-axis without penetrating each other. Because during folding all triangles move inwards, this condition is most severe in the fully folded state where it can be shown that

$$\frac{l_b}{l_a}\le\frac{\sin\dfrac{(n-2)\pi}{2(m+n)}}{\sin\dfrac{(m+2)\pi}{2(m+n)}}. \tag{14}$$

The equality sign corresponds to the c sides lying along diameters of the coordinate cylinder.

3 Folding Properties

The results of Section 2 can be used to select particular layouts of triangulated cylinders which are suitable for folding, i.e., where both the extended and folded configurations are strain-free, and to gain insight into the folding process. A key assumption is made, that the folding process is uniform, i.e., that all triangles remain identical throughout the folding process. This assumption may appear rather restrictive, particularly because Fig. 1 shows clearly that the deformation pattern in any partially packaged configuration is not uniform: it consists of a fully folded region, at the top, of a fully extended region, at the bottom, and of an intermediate "transition" region. If any strains are induced by folding, one would expect them to be in the transition region and, obviously, this localization cannot be captured if it is assumed that all triangles remain identical. This restriction has been removed in a separate investigation (Guest and Pellegrino, 1994).

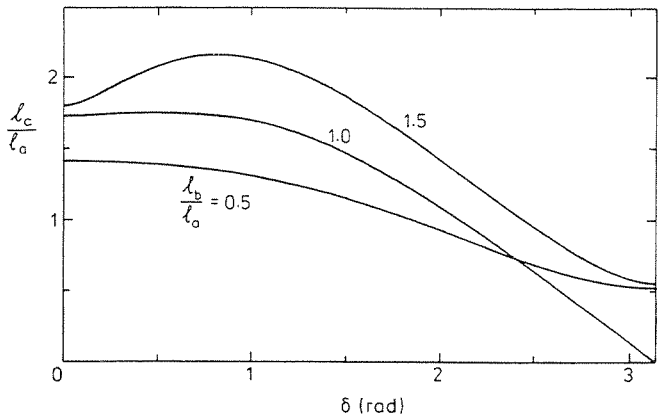

Fig. 6(*a*)

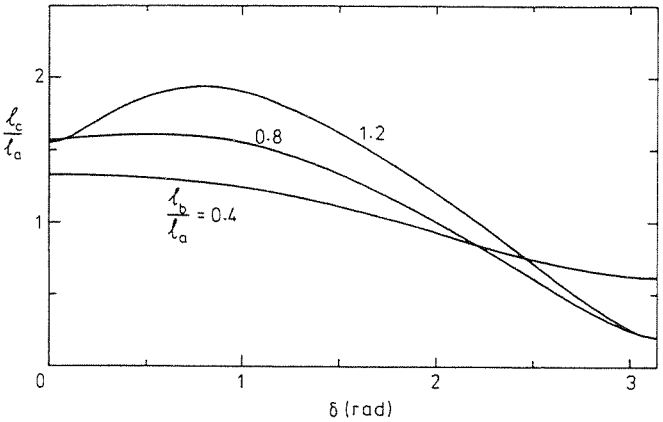

Fig. 6(*b*)

Fig. 6 Plots of l_c/l_a versus δ for triangulated cylinders with (*a*) $m=1$ and (*b*) $m=2$; $n=7$ in both cases

The simplest way of approaching the problem is to investigate the geometric configurations of cylinders with $l_b/l_a=$ constant. This is equivalent to assuming that all deformation can be modeled in terms of changes of l_c only. With these hypotheses, the folding properties of any particular type of triangulated cylinder, defined by l_b/l_a, m, and n can be investigated most effectively on a plot of l_c/l_a versus δ, where

$$\delta=\beta-\alpha \tag{15}$$

(see Fig. 4). Obviously, $0\le\delta<\pi$: configurations with $\delta=0$ have zero height and will be referred to as fully folded. All plots presented in this section have been obtained by solving numerically the nonlinear system of four Eqs. (11)-(13), (15) for the four unknowns r/l_a, α, β, and l_c/l_a, given l_b/l_a, m, n, and δ. The function "fsolve," available in Matlab (The Math Works, 1989), has been used. No closed-form solution has been searched for.

Figure 6(*a*) shows a plot of l_c/l_a versus δ for triangulated cylinders with $m=1$, $n=7$ and for three different values of l_b/l_a. Consider initially the case $l_b/l_a=0.5$. The figure shows that l_c decreases monotonically as δ increases. Indeed, this is the type of behavior that would be expected if all triangles were in a plane, rather than being wrapped in a tube. Within obvious limits, any value of l_c/l_a is associated with a unique configuration of the cylinder. The case $l_b/l_a=1$ (isosceles triangles) is much more interesting since now l_c/l_a initially increases with δ and then, having reached a maximum, starts

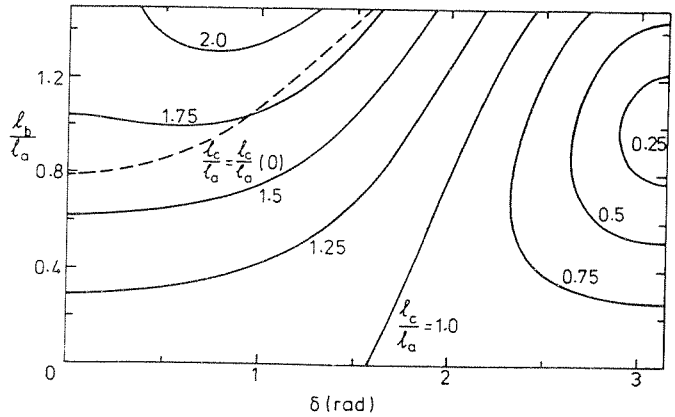

Fig. 7(a)

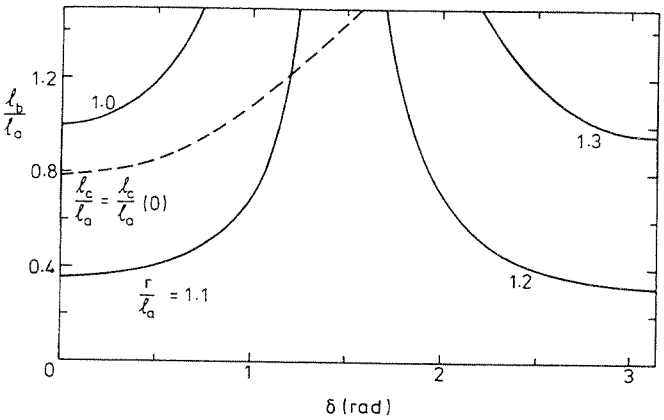

Fig. 7(b)

Fig. 7 Contour plots of (a) l_c/l_a and (b) r/l_a for triangulated cylinders with $m=1$ and $n=7$

decreasing. This can be explained by the effect of the curvature of the cylindrical surface, on which all corner nodes lie, becoming significant. In this case any triangulated cylinder with $l_c/l_a \geq \sqrt{3}$ admits two different, totally unstrained configurations. In particular, $l_c/l_a=\sqrt{3}$ gives one configuration where $\delta=0$ and one where $\delta=0.867$. This is the same cylinder which has been analyzed, by much simpler means, in the Introduction. The third curve in Fig. 6(*a*), for the case $l_b/l_a=1.5$ shows similar behavior, but this time there is a much more marked maximum. This curve shows that triangulated cylinders with $l_b/l_a=1.5$ and $l_c/l_a=1.800$ are strain-free both when fully folded ($\delta=0$) and when extended ($\delta=1.587$); however, going from one configuration to the other requires large deformations.

Similar considerations apply to other triangulated cylinders. For example, Fig. 6(*b*) shows similar curves for the case $m=2$, $n=7$. Note that the three curves in this figure refer to lower values of l_b/l_a than in the case $m=1$ because the upper limit on l_b/l_a, Eq. (14), is a little lower.

A more general way of plotting data for the case $m=1$, $n=7$ is a contour plot of l_c/l_a for the full range of δ and l_b/l_a, Fig. 7(*a*). A broken line marks those configurations of the cylinder which admit also a strain-free folded configuration with $\delta=0$. These are the configurations on which we are focusing in this paper. The value $l_b/l_a=0.788$ is the lowest possible for fully foldable cylinders. Also note that the contour $l_c/l_a=1.75$, for example, indicates that cylinders with $l_b/l_a=1.039$ require fairly small strains to go from $\delta=0$ and $\delta=0.940$ because the dimple in the contour is rather flat. The contour $l_c/l_a=1.64$ (not shown) is even flatter, thus allowing δ to vary in the range 0–0.4 with less than 0.1 percent variation in l_b/l_a. Finally, note that the upper limit on l_b/l_a is 1.497, from Eq. (14). Figure 7(*b*) plots the corresponding values of r/l_a: folding, i.e., decreasing δ always implies a reduction of r.

4 Discussion

The general geometric formulation of Section 2 together with the sample plots presented in Section 3 are very powerful tools for the design of foldable tubes. With this approach one can go well beyond the fairly intuitive foldable cylinders presented in the Introduction, all of which had $m=1$ and $l_b/l_a=1$. Obviously, having the freedom to alter these two parameters can be very useful in the design of foldable cylinders that have to meet some specified requirements. With the hypothesis that l_a and l_b remain constant during folding, while l_c varies, preliminary estimates of strains during folding are easy to obtain (see Fig. 6). More detailed estimates of strains, axial force, shape and length of transition region, etc., are available in Guest and Pellegrino (1994).

Although this paper has concentrated on cylinders which are strain-free both when fully deployed and fully packaged, it should be noted that it is also possible to design cylinders which accumulate elastic strain energy during folding and release it during deployment. This property could be useful for some particular applications, e.g., self-deploying cylinders.

An interesting feature of the plots in Fig. 6 is that they identify some special triangulated cylinders whose l_c/l_a is an analytical maximum. For example, the special configuration of a cylinder with $m=1$, $n=7$ and $l_b/l_a=1.5$ occurs for $\delta=0.839$ and hence $l_c/l_a=2.162$ (see Fig. 6(*a*)). Any cylinder made to be strain-free in such a configuration can change its δ by an infinitesimal amount without any first-order changes of length in the triangular panels. Indeed, Calladine's model, referred to in Section 1, had this property and our analysis has produced a whole group of cylinders with the same property as a by-product. It is well known, see Calladine (1978) for example, that special, singular configurations of an assembly of pin-jointed bars are obtained when the length of one bar, or a group of bars, is maximum. One might expect that the configurations corresponding to the maxima of Fig. 6 should have such property, but they do not. This is because only uniform configurations were considered in the analysis leading to the plots in Fig. 6 and hence the maxima of l_c/l_a are, indeed, the largest when this constraint is enforced. However, if this constraint is removed nonuniform configurations with larger l_c/l_a can be obtained. This has been verified by careful computations based on Pellegrino (1993).

Acknowledgments

We thank Prof. C. R. Calladine for advice and comments on an earlier version of this paper, and Mr. S. Vincer of ITW Irathane International for assistance in the manufacture of the model shown in Fig. 1. We acknowledge, with thanks, financial support from British Aerospace (Space Systems) Ltd. and SERC (S.D.G.), and the award of ESA Fellowship (S.P.).

References

Calladine, C. R., 1978, "Buckminster Fuller's Tensegrity Structures and Clerk Maxwell's Rules for the Construction of Stiff Frames," *International Journal of Solids and Structures*, Vol. 14, pp. 161–172.

Coxeter, H. S. M., 1980, *Introduction to Geometry*, 2nd ed., John Wiley and Sons, New York.

Guest, S. D., and Pellegrino, S., 1992, "Inextensional Wrapping of Flat Membranes," *Proc. First International Seminar on Structural Morphology*, R. Motro and T. Wester, eds., Montpellier, La Grand Motte, pp. 203–215.

Guest, S. D., and Pellegrino, S., 1994, "The Folding of Triangulated Cylinders, Part II: The Folding Process," ASME JOURNAL OF APPLIED MECHANICS, Vol. 61, pp. 778–783.

Kwan, A. S. K., 1991, "A Pantographic Deployable Mast," Ph.D. dissertation, University of Cambridge, Cambridge, U.K.

Kwan, A. S. K., You, Z., and Pellegrino, S., 1993, "Active and Passive Cable Elements in Deployable Masts," *International Journal of Space Structures*, Vol. 8, pp. 29–40.

Pellegrino, S., 1993, "Structural Computations with the Singular Value Decomposition of the Equilibrium Matrix," *International Journal of Solids and Structures*, Vol. 30, pp. 3025–3035.

The Math Works, 1989, Matlab User's Guide.